

Cytoskeletal Priming of Mesenchymal Stem Cells to a Medicinal Phenotype

Amr A. Abdeen¹ · Junmin Lee¹ · Yanfen Li² · Kristopher A. Kilian^{1,2}

Received: 24 August 2016 / Accepted: 19 December 2016 / Published online: 6 January 2017
© The Regenerative Engineering Society 2017

Abstract

Mesenchymal stem cell (MSC) therapy is a promising approach for the treatment of cardiovascular disease, demonstrating pronounced trophic, immunomodulatory, and pro-angiogenic activity. However, clinical efficacy has suffered from broad variability, presumably due to cell death upon implantation, and the heterogeneous population of autologous cells. Micropatterning single cells in the same geometry can normalize the phenotype in a population, and variations in subcellular curvature will guide focal adhesion, cytoskeletal organization, and the regulation of distinct epigenetic marks to orchestrate a medicinal secretome. Within 2 days, activated cells show elevated expression of pericyte markers and will recapitulate functional pericyte activity through enhanced association with endothelial cell tubules in co-culture. MSCs are believed to undergo a temporary switch *in vivo* to an activated state in response to injury; thus, we propose engineering actomyosin contractility after isolation can similarly activate MSCs, which may serve as a general approach to prime a medicinal phenotype for cell-based therapies.

Lay Summary

Patient-derived mesenchymal stem cells will secrete molecules that promote new vasculature and have demonstrated clinical efficacy as a therapy for treating myocardial infarction. While autologous cell implantation is promising, there is considerable variability in current treatments and controversy over the underlying mechanisms. In this work, we reveal that careful control of actomyosin contractility in mesenchymal stem cells can prime a pericyte state with a medicinal secretome that shows sustained pro-angiogenic activity *in vitro* and *in vivo*. Activation of mesenchymal stem cells to a medicinal phenotype may increase the efficacy and reproducibility of cell-based therapies for cardiovascular disease

Keywords Mesenchymal stem cells · Micropatterning · Actomyosin contractility · Pericyte · Angiogenesis

Introduction

Cardiovascular disease is the number one cause of death in the United States accounting for about a third of all mortalities [1]. Angiogenesis therapy, aiming to stimulate blood vessel growth from pre-existing vessels, is a proposed solution for several cardiovascular conditions including myocardial infarction [2, 3]. However, angiogenesis is a very complex process involving multiple mechanisms working in tandem [4], and treatments like cytokine delivery often cause unwanted effects such as aberrant vascularization [5]. The use of autologous cells is a promising alternative [6] because of the low risk of rejection and the temporally regulated secretion of trophic, immunomodulatory, and pro-angiogenic molecules. In

A.A.A. and J.L. contributed equally to this work.

Electronic supplementary material The online version of this article (doi:10.1007/s40883-016-0021-8) contains supplementary material, which is available to authorized users.

✉ Kristopher A. Kilian
kakilian@illinois.edu

¹ Department of Materials Science and Engineering, University of Illinois at Urbana-Champaign, Urbana, IL 61801, USA

² Department of Bioengineering, University of Illinois at Urbana-Champaign, Urbana, IL 61801, USA

particular, mesenchymal stem cells (MSCs) are a leading candidate for implantation to promote angiogenesis [7].

MSCs are mesoderm-derived, multipotent adult stem cells with the ability to differentiate into multiple cell types [8]. Although MSCs have been reported to differentiate into endothelial cells [9] and specify toward a cardiomyocyte lineage [10], they show limited long-term engraftment [11]. The dominant therapeutic role of MSCs is proposed to be secretion of paracrine signals *in vivo* [12]. This is unsurprising considering the strong evidence for a perivascular origin for MSCs, with perivascular cells exhibiting MSC features *in vitro* after long-term culture including the ability to differentiate to the same lineages [13–17]. In fact, co-culturing MSCs with endothelial cells may stabilize engineered vasculature *in vivo* for several months [18].

The therapeutic potential of MSCs, however, is very dependent on the context in which they are used and understanding how it is regulated is critical. For example, preconditioning is a potent way to increase MSC survival, engraftment, and angiogenesis outcomes after injection. In addition, encapsulation of MSCs in synthetic or natural biomaterials supports MSC survival and their properties can influence therapeutic performance, although the mechanisms are not completely understood [7]. Extracellular matrix (ECM) properties are some of the most potent regulators of MSC behavior. For example, combinations of biophysical and biochemical cues will affect MSC differentiation [19–21], while merely altering cell shape can affect differentiation [22] or multipotency and quiescence [23]. During injury, there are many changes to the ECM both through external factors and through cell-based remodeling of the extravascular space, and these changes provide a rich signaling environment to guide cellular activities. We have previously shown that ECM changes can affect the pro-angiogenic potential of MSCs *in vitro* [24], with a maximum response occurring when MSCs are fully spread on relatively stiff fibronectin conjugated matrices. Deciphering the role of extracellular signals that guide MSC state and pro-angiogenic potential is imperative to ensuring reproducible efficacy during cell-based therapies.

Accompanying changes in the ECM, cells in the perivascular space are also transformed during injury. These transformations are difficult to study as cell identity *in vivo* is dynamic with significant overlap between different populations in the perivascular space. This complicates finding and targeting specific populations for therapy. An alternative would be identifying master regulators which may act to promote pro-angiogenic states in multiple cell populations to work in concert in healing. Two well-known such regulators of angiogenesis are hypoxia [25] and vascular endothelial growth factor (VEGF) [26]. Cytoskeletal organization and actomyosin contractility is regulated in multiple cell types during angiogenesis. Endothelial cell organization and angiogenesis [27] is Rho-activity dependent, fibroblasts form stress

fibers and express contractile proteins such as alpha smooth muscle actin (α -SMA) during wound healing [28, 29], and pericytes' contractility influences sprouting and proliferation of endothelial cells [30, 31]. We hypothesized that MSC pro-angiogenic behavior would similarly be enhanced through cytoskeletal manipulation.

In this paper, we show that engineering the cytoskeletal tension of single MSCs will modulate the epigenetic state and prime a pro-angiogenic “medicinal” phenotype. Primed MSCs demonstrate enhanced secretion of angiogenic cytokines and association with endothelial cells in co-culture. Analysis of molecular markers suggests a switch from multipotent stem cell to a pericytic state that promotes angiogenic remodeling, the targeting of which may provide a more systematic way to optimize physical properties of biomaterials for translation. We propose that this approach will also serve as a physical preconditioning step to “activate” MSCs prior to autologous therapy.

Materials and Methods

All reagents were purchased from Sigma Aldrich unless otherwise stated. Cell culture reagents and antibodies used are listed in [Supplementary Table S1](#).

Gel Fabrication and Micropatterning

Patterned 40-kPa PA hydrogels were made as described previously [20]. Briefly, 0.01% ammonium persulfate and tetramethylethylenediamine are mixed into an 8% acrylamide and 0.48% bis-acrylamide solution to initiate gelation. 20 μ l of the mixture is pipetted between a hydrophobic slide (treated with RainX) and an activated coverslip treated with 0.5% aminopropyl(trimethoxy silane) for 3 min, washed thoroughly, and then treated with 0.5% glutaraldehyde for 30 min. After 20 min, the gel is detached and treated with 55% hydrazine hydrate for 2 h on a rocker and then washed with 5% glacial acetic acid and DI water and stored for later use. PDMS stamps with desired features were made from silicon masters made by conventional photolithography and fibronectin (25 μ g/mL treated with 3.5 mg/mL sodium periodate for at least 30 min to oxidize sugar groups into aldehydes) was pooled on the surface of the stamps for 30 min and then stamped onto the surface of partially dried hydrogels to form the desired fibronectin patterns.

Cell Source and Culture

MSCs were obtained from Lonza and were harvested and cultured from normal bone marrow. Cells were positive for CD105, CD166, CD29, and CD44 and negative for CD14, CD34, and CD45 by flow cytometry (<http://www.lonza>.

com). MSCs were cultured in low glucose (1 g/mL) DMEM (10% FBS and 1% penicillin/streptomycin) and human microvascular endothelial cells (hMVECs) (Cell Systems) were cultured in EGM-2 media (Lonza). Cells were passaged at approximately 80% confluency and media was changed every 3–4 days. Cells were used at passages 4–10. Cells were trypsinized using 0.25% Trypsin and MSCs were seeded on surfaces at ~ 5000 cells/cm². MSCs were cultured for 2 days on patterned or non-patterned surfaces, and their conditioned media was collected and used directly (without freezing) for tubulogenesis assays.

For inhibition studies, Blebbistatin (1 μ M) and Y-27632 (2 μ M) or integrin blocking antibodies $\alpha_5\beta_1$ and $\alpha_v\beta_3$ (1 μ g/mL) were added to the MSC media or blocking antibodies (VEGF, IGF, and RANTES) were added to conditioned media as per manufacturer's instructions for effective blocking.

Cell Fixing, Staining, and Imaging

Cells were fixed using 4% paraformaldehyde for 20 min after rinsing twice with PBS. Then 0.1% Triton X-100 was used to permeabilize the cells for 30 min. Cells were blocked using 1% bovine serum albumin and then stained with the appropriate primary and secondary antibodies (Supplementary Table 1). DAPI (1:4000) and Alexa 488-phalloidin (1:200) were used to image nuclei and actin, respectively. Imaging was done using a Zeiss Axiovert 200M inverted fluorescence microscope or an IN Cell Analyzer 2000 (GE healthcare) for fluorescence imaging or an LSM 700 (Carl Zeiss, Inc.) four laser point scanning confocal microscope with a single pinhole for confocal imaging.

For co-culture experiments, red and green cell tracker (Invitrogen) were used on hMVECs and MSCs, respectively, as per manufacturer instructions. Cells were fixed as above (without permeabilization) and imaged.

In Vitro Tubulogenesis Assay

The in vitro vascularization assay was performed as described previously [24]. Briefly, 25 μ L of thawed reduced growth factor matrigel (Trevigen) was used to coat the bottoms of 48-well plates and then allowed to gel for 30 min at 37 °C. Then, 15,000 hMVECs were seeded per well in 100 μ L of unsupplemented EBM-2 media (Lonza) and 400 μ L of MSC conditioned media was added to each well. Unsupplemented EBM-2 media was used as a negative control while fully supplemented EGM-2 was used as a positive control. After 8 h, tube formation was imaged using a Rebel T3 Camera (Canon) at $\times 25$ and tube area quantified using ImageJ. For co-culture experiments, primed MSCs were additionally seeded at 5000 cells/well.

Angiogenic Cytokine Array

For cytokine analysis in the conditioned media, we used human antibody angiogenesis array membrane (Abcam—ab134000) as per manufacturer instructions. Membranes were blocked and then conditioned media samples were incubated overnight with the membranes at 4 °C. Prepared membranes were exposed to x-ray film for detection and, after development, films were scanned and analyzed using the ImageJ plugin “Protein array analyzer” (written by Gilles Carpentier, 2010, available at <http://rsb.info.nih.gov/ij/macros/toolsets/Protein%20Array%20Analyzer.txt>)

Chick Chorioallantoic Assay

Embryonated chicken eggs at day 10 were obtained from the University of Illinois poultry farm (Urbana, IL). A hole with approximate width of 15 mm was drilled and polyacrylamide hydrogels with MSCs seeded on it in patterned or non-patterned conditions were placed on the chorioallantoic membrane (CAM), face down. The hole was covered with scotch tape and the eggs were incubated for 5 days at 37 °C and $\sim 50\%$ humidity. On the fifth day after incubation, embryos were fixed with 4% PFA and the hydrogels and surrounding CAMS were excised. The explants were imaged and the area covered with blood vessels over the gels was quantified using ImageJ as for the in vitro tubulogenesis assays as described above.

Data Analysis and Statistics

Cell area, nuclear area, and marker expression levels were analyzed using ImageJ. MSC/hMVEC overlap area was performed by thresholding fluorescent images of cell-tracked MSCs and hMVECs and using the ImageJ image calculator's “AND” operation to get the overlapping area. Error bars represent standard error and *N* value the number of experimental replicates. Unpaired *T* tests were used to compare two groups while ANOVA was used to compare multiple groups with Tukey HSD post hoc analysis. *P* values lower than 0.05 were considered significant.

Results

Tuning the Pro-Angiogenic Potential of Mesenchymal Stem Cells Through Single-Cell Contractility Engineering

Previously, we demonstrated optimal matrix properties to guide the pro-angiogenic potential of MSCs, where cell spread area on rigid matrices conjugated with fibronectin played a key role in augmenting secretion of pro-angiogenic molecules on 40 kPa polyacrylamide (PA) hydrogels [24]. However, in vivo, cells are surrounded by the extracellular matrix, and

the spreading characteristics of MSCs observed on planar substrates are not observed. Therefore, we asked whether patterning single cells within the same footprint, in geometries presenting different degrees of subcellular adhesive space, could be used to modulate cytoskeletal tension in the absence of spreading. We employed microcontact printing of fibronectin islands onto hydrazine hydrate treated polyacrylamide hydrogels to facilitate covalent conjugation. After MSCs are cultured for 2 days in the desired geometries, MSC conditioned medium is collected and added to hMVECs on matrigel for 8 h, after which the amount of tube formation by hMVECs is quantified as a measure of the pro-angiogenic potential of the MSC culture conditions (Fig. 1a).

We utilized three different shapes of relatively small area ($3000 \mu\text{m}^2$) to ensure that cells are not fully spread, a pentagon

and two 5-pointed stars presenting variable subcellular adhesive area. The points of the star span non-adhesive space (~ 500 and $1250 \mu\text{m}^2$), causing increased cytoskeletal tension as demonstrated by reinforcement of peripheral actin and formation of stress fibers [32], and increased stability of focal adhesion at apexes. Vinculin heat maps demonstrate increased focal adhesion area at the points of the shapes as the non-adhesive space increases (Fig. 1b). Similar trends were observed for focal adhesion protein paxillin, $\alpha_5\beta_1$ and $\alpha_v\beta_3$ integrins, and myosin IIb (Fig. S1). Cells attached to the patterns at approximately the same fraction and exhibited similar projected cell areas (Fig. S2).

Conditioned media collected from MSCs cultured in these shapes was used to promote tubulogenesis in hMVECs cultured in matrigel. Tube formation shows a

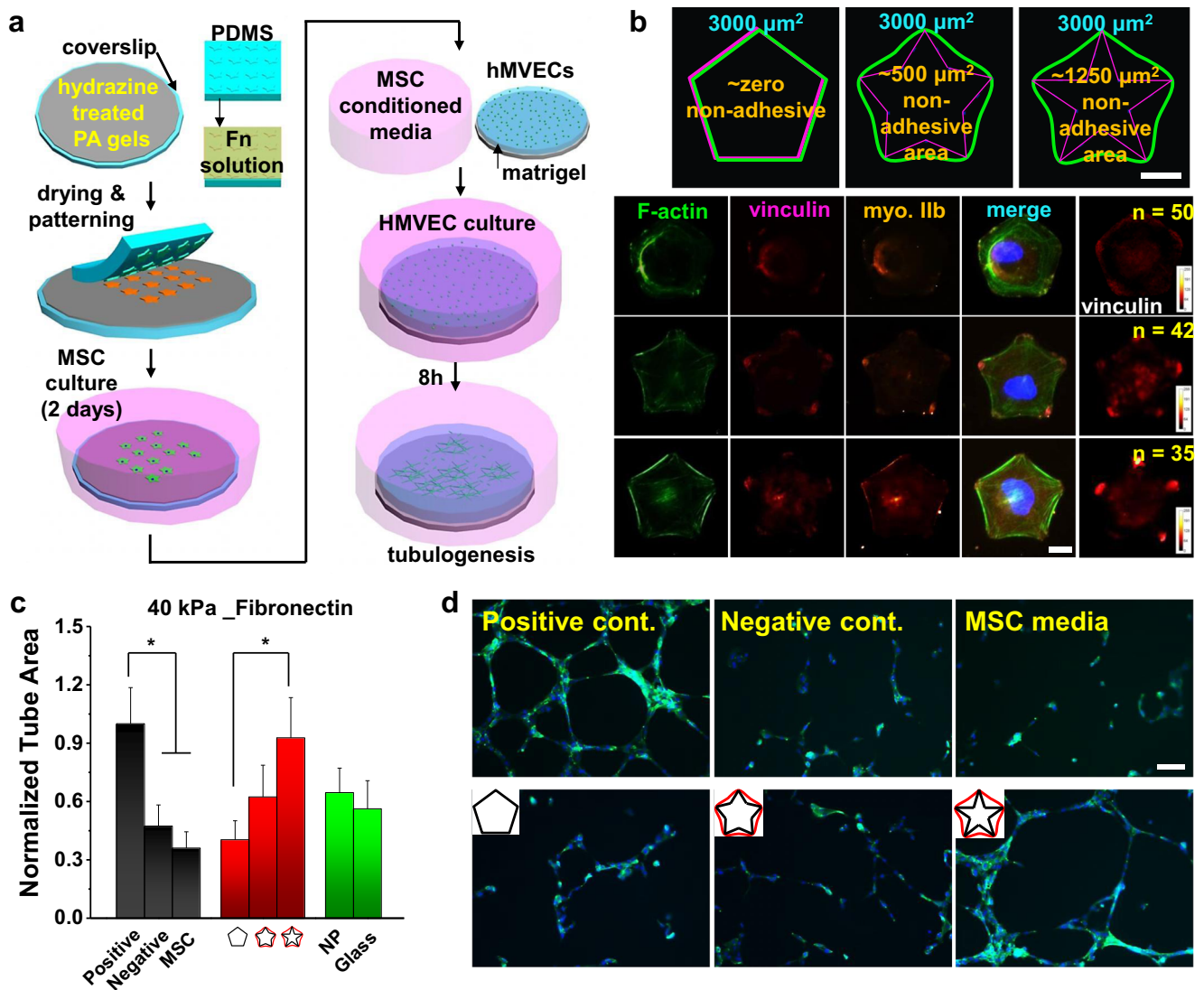


Fig. 1 Patterning modulates MSC cytoskeletal tension to influence pro-angiogenic potential. **a** Experimental procedure for micropatterning MSCs and in vitro tubulogenesis assay. **b** Focal adhesion and cytoskeletal staining of MSCs cultured on patterns with increasing non-adhesive

areas. *Scale bar*: 25 μm . **c** Tube area formed by hMVECs after being treated with conditioned media from MSCs patterned with increasing non-adhesive areas ($N = 6$). **d** Representative images of hMVEC tube formation at different conditions. *Scale bar*: 100 μm . * $P < 0.05$

dependence on the non-adhesive area upon which cells are patterned (Fig. 1c, d), with conditioned media from star-shaped MSCs showing the highest degree of tubulogenesis as compared to our positive controls (hMVEC growth media). hMVEC cultures supplemented with conditioned media from star-shaped MSCs show ~2-fold higher tube formation compared to cells cultured on pentagon patterns. We also evaluated the influence of cellular elongation on secretion to support the results of our pentagonal shaped cells since changes in aspect ratio have previously been demonstrated to increase cytoskeletal tension [22]. Tube formation assays demonstrate increasing pro-angiogenic potential as MSCs are cultured within shapes of increasing aspect ratio (Fig. S3), peaking at 1:8 and decreasing at 1:12, presumably as elongation beyond 1:8 destabilizes the cytoskeleton [33].

Overall, this data indicates a strong correlation between the apparent cytoskeletal tension of MSCs and their secretion of pro-angiogenic cytokines. This is not the case, however, when comparing to MSCs on glass substrates which, while having the largest spread areas and most robust stress fibers, show little enhancement to MSC pro-angiogenic potential. This demonstrates the importance of studying cells at more physiologically relevant conditions. In order to further understand the process, we looked at how the angiogenic secretome of MSCs was modulated by engineering actomyosin contractility.

The Influence of Single-Cell Contractility on the Secretome

Protein arrays were used to investigate the influence of cytoskeletal tension on the pro-angiogenic secretory profile of MSCs. The relative concentrations of a panel of 20 different angiogenic cytokines in MSC conditioned media were compared. To simplify the analysis, we compared cytokines secreted by MSCs patterned on pentagonal shapes to those patterned in star shapes which had the largest cytoskeletal tension. Figure 2a shows a heat map of protein expression normalized to cell number. We see an increase in expression of pro-angiogenic proteins secreted from star-patterned MSCs across the broad spectrum of cytokines compared to molecules secreted from pentagon-patterned MSCs. For further study, we selected three of the most potent angiogenic regulators with the highest differential expression between pentagon and star MSCs, namely IGF-1, RANTES, and VEGF (Fig. 2b) to investigate their effects on hMVEC tube formation. The addition of function blocking antibodies to MSC conditioned medium targeting any of these factors lowered hMVEC tube formation from star-patterned MSCs; only a modest decrease was observed from pentagon-patterned MSCs (Fig. 2c). Suppression of a single factor decreases

angiogenesis considerably, even in the presence of other factors, suggesting the importance of synergy during promotion of angiogenesis.

Activation of Mesenchymal Stem Cells to a Pericyte State

Since the contractility state of MSCs influences the secretome, we sought to investigate the putative phenotypic switch through changes in expression of a panel of markers: MSC multipotency marker endoglin/CD105, the pericyte and activated fibroblast marker α -SMA [34], CD146 [13] as a pericyte marker that is used to separate MSCs from pericytes, and RGS-5 [35]. RGS-5 is also upregulated during activation of pericytes through neovascularization and wound healing [36]. Immunofluorescence imaging and quantitation of average marker intensity (Fig. 2d, e) show an ~1.5-fold increase in α -SMA and CD-146 expression and a ~1.25-fold increase in RGS-5 expression from pentagon to star, along with a slight decrease in endoglin expression (~20%). Taken together, this suggests that MSCs initiate secretion of angiogenic molecules through adoption of an activated pericyte-like state via a process mediated by cytoskeletal tension. Notably, MSCs cultured on non-patterned (NP) surfaces and glass demonstrate low expression of these markers compared to patterned MSCs.

Previously, it was shown that isolated pericytes adopt MSC characteristics during culture on rigid substrates *in vitro* [13, 15]. The converse appears to be true here, where MSCs cultured on patterned hydrogels express elevated pericyte markers. Elevated endoglin expression in pentagon-patterned MSCs may be consistent with increased quiescence [23], although the degree of change in expression is low. Higher CD146 expression in star-patterned MSCs is especially telling since CD146 is a particularly robust pericytic marker. In fact, Raghunath et al. [37] have shown pro-angiogenic and pericytic activity of sorted CD146+ MSCs but not CD146- MSCs. Furthermore, increased RGS-5 expression is consistent with both a more pericytic state and increased angiogenic activity.

In order to confirm the role of actomyosin based cytoskeletal tension in pericyte activation, we added the RhoA activator lysophosphatidic acid (LPA) [38] to MSCs cultured in pentagon patterns, and Blebbistatin (inhibitor of myosin II) and an inhibitor of Rho-associated protein kinase (ROCK; Y27632) to MSCs cultured in star patterns. Immunofluorescent staining of myosin IIb shows ~35% increases in myosin IIb intensity in LPA-treated MSCs in pentagon shapes giving comparable intensity to MSCs in star patterns. Blebbistatin and Y27632, on the other hand, showed a modest decrease in myosin IIb intensity compared to controls: ~15% and 23% lower, respectively (Fig. S4). Treatment of pentagon-patterned MSCs with LPA leads to a more than 3-fold increase in tube

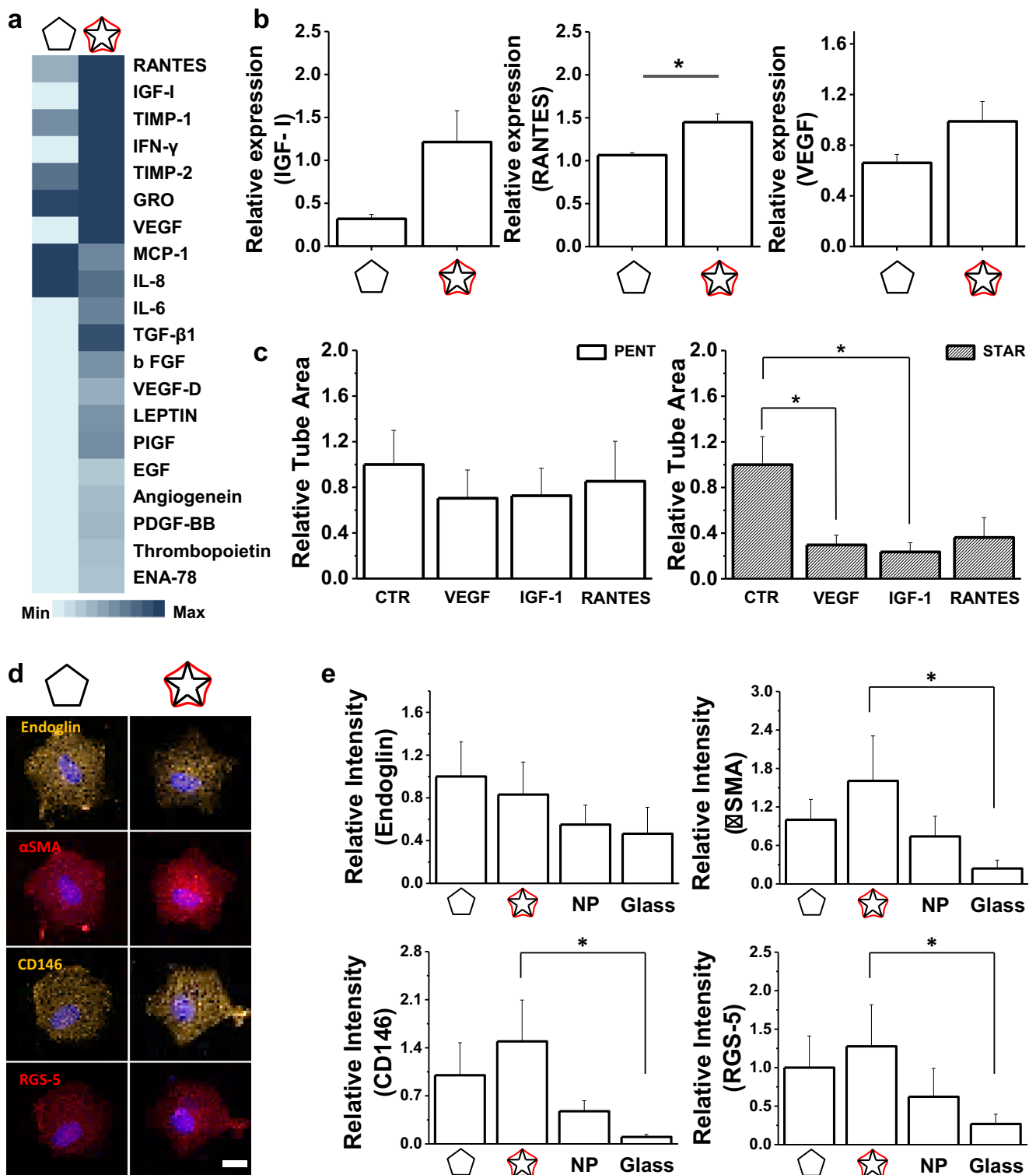


Fig. 2 MSC cytoskeletal tension modulates the secretome and activates a pericytic state. **a** Heat map of cytokine expression in conditioned media of MSCs cultured in pentagon or star patterns, shown as fold change over the non-patterned condition. **b** Relative expression (fold change over NP) of IGF-1, RANTES, and VEGF. **c** Effect of adding blocking antibodies to

IGF-1, RANTES, and VEGF to MSC conditioned media on tube formation of hMVECs. **d** Representative immunofluorescence images of patterned MSCs showing Endoglin/CD105, α -SMA, CD146, and RGS-5 expression in pentagon and star geometries. **e** Average marker intensities relative to the pentagon condition. Scale bar: 25 μ m. * $P < 0.05$

formation from MSC conditioned media while Blebbistatin and Y27632 treatment of MSCs in star

shapes caused a modest decrease of ~35% in tube formation (Fig. 3a). Blocking of $\alpha_5\beta_1$ and $\alpha_v\beta_3$ integrins using

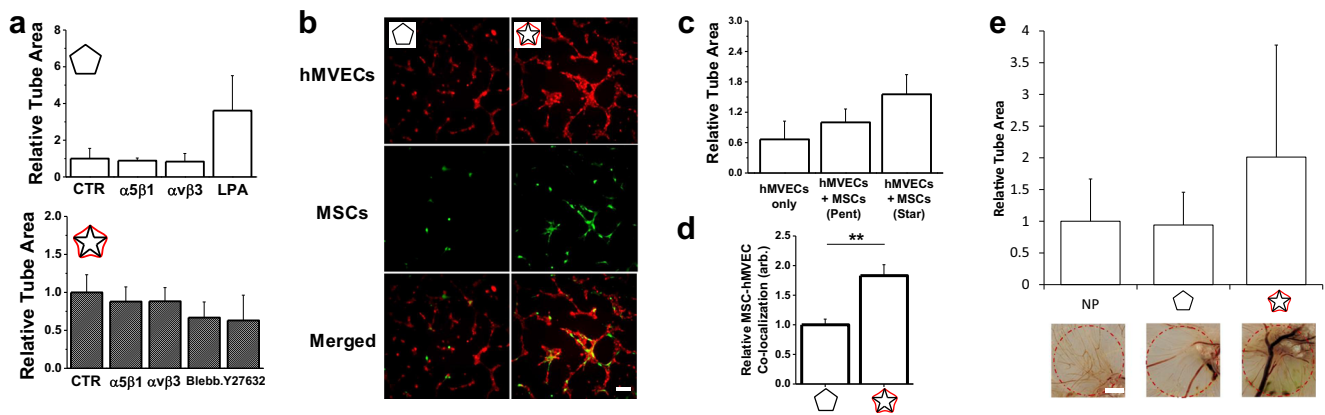


Fig. 3 Activated MSCs exhibit pericytic behavior in co-culture with endothelial cells and enhance in ovo angiogenesis. **a Top**—effect of treatment of pentagon-patterned MSCs with blocking antibodies to integrins $\alpha_5\beta_1$ and $\alpha_v\beta_3$ or LPA to enhance contractility ($N = 5$). **Bottom**—effect of treatment of star-patterned MSCs with blocking antibodies to integrins $\alpha_5\beta_1$ and $\alpha_v\beta_3$ or Blebbistatin and Y27632 to reduce contractility ($N = 3$). **b** Representative immunofluorescence images of hMVEC tube formation (red) and MSCs (green) when co-cultured on matrigel for 8 h.

function blocking antibodies did not play a significant role on the angiogenic potential of either pentagon-patterned or star-patterned MSCs. With MSCs adopting an activated pericyte-like state by confinement, we asked whether cytoskeletal engineering through patterning was affecting the epigenetic state of MSCs.

Activated Mesenchymal Stem Cells Associate with Vascular Endothelial Cells in Co-Culture

To explore how activation may influence heterotypic interactions in culture, we passaged pentagon-patterned and star-patterned MSCs for 2 days then trypsinized and co-cultured them with hMVECs. An in vitro angiogenesis assay was performed and tube formation and MSC localization on tubes were analyzed after 8 h (when maximum tube formation is observed) via cell tracker. Representative images of the formed tube networks with pentagon-patterned and star-patterned MSCs show higher tube formation with higher association of MSCs (with MSCs spreading along the tubes) for star-patterned MSCs (Figs. 3b and S5). Quantitation of tube area shows a 1.5-fold increase in tube formation when MSCs are cultured on star rather than pentagon geometries prior to co-culture (Fig. 3c). Both conditions show higher tube formation than lone hMVECs. Furthermore, MSC coverage of the tubes was ~ 1.8 times higher in star than pentagon (Figs. 3d and S5).

Although there have been several reports of MSC-endothelial cell co-cultures, only a subset explore the effect of preconditioning MSCs on their behavior in co-culture [7]. Here, we observe a pronounced effect of preconditioning on MSC-hMVECs interactions, highlighting the

importance of considering MSC culture conditions prior to therapeutic use. Since broad changes in the secretome and association with endothelial cells indicated a more directed switch in MSC behavior, we then looked into changes in MSC state.

In Ovo Pro-Angiogenic Potential of Activated MSCs

Activating MSCs through patterning shows evidence of pro-angiogenic potential in vitro; next, we explored whether activated MSCs will demonstrate pro-angiogenic activity in vivo using a chick chorioallantoic membrane (CAM) [39] assay, in the presence of existing vascular networks. We placed hydrogel patches containing non-patterned, star-patterned, or pentagon-patterned MSCs on the CAMs of 10-day-old chick embryos and analyzed the formation of new vessels after 5 days (Fig. 3e). We see enhanced vessel formation in CAMs after administration of star-patterned MSCs, when compared to pentagon patterned and non-patterned MSCs, with vessels that are much bigger and more mature being formed on CAMs supplemented with star-patterned MSCs. This demonstrates that activated MSCs show an enhanced pro-angiogenic phenotype when applied to the in ovo CAM system, thereby providing evidence that cytoskeletal priming may prove a route to increasing the efficacy of MSC pro-angiogenic therapy.

Mesenchymal Stem Cell Activation Is Regulated Through Histone State

Cell activity is regulated through modifications of specific histone marks, with cytoskeletal tension playing a role in

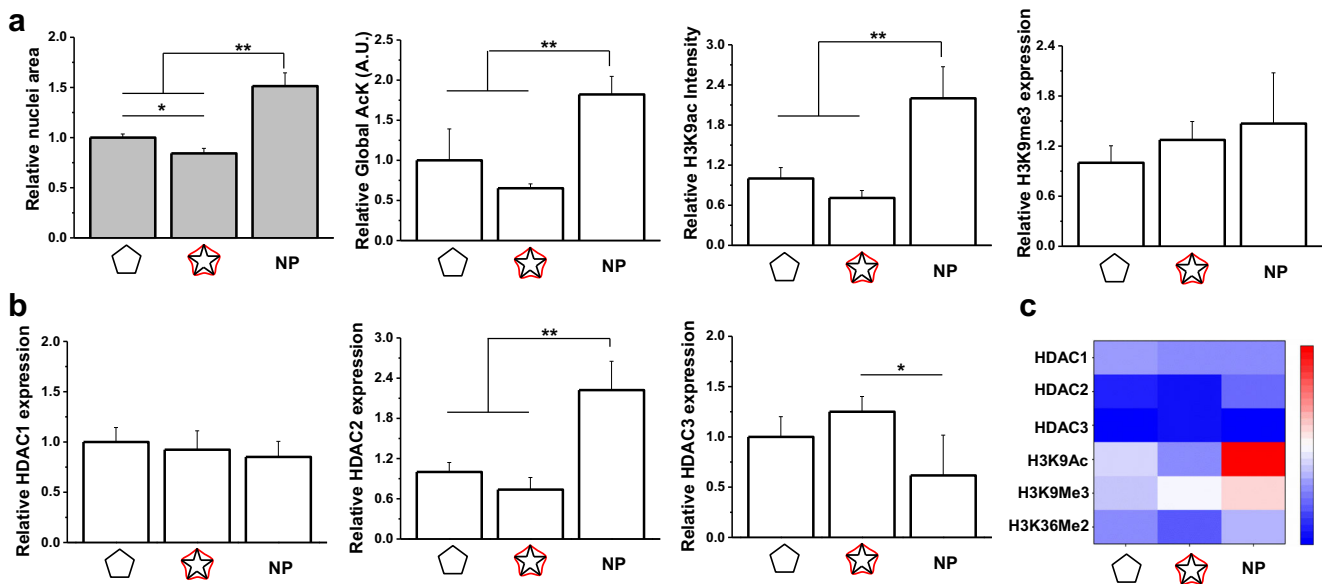


Fig. 4 Histone state regulates mesenchymal stem cell activation. **a** Relative nuclear area between non-patterned, pentagon-shaped, or star-shaped MSCs and relative intensity of global acetylated lysine, H3K9 acetylation or H3K9 trimethylation. **b** Relative expression of HDACs 1,

2, and 3. **c** Heat map comparing the chromatin modification markers across non-patterned, pentagon-shaped, or star-shaped MSCs. * $P < 0.05$, ** $P < 0.01$

guiding nuclear organization [40, 41], chromatin structure, and gene expression [42, 43]. Analysis of nuclear area for patterned and non-patterned MSCs demonstrates a significant decrease in nuclear area of both pentagon-patterned and star-patterned MSCs (Fig. 4a); hence, we suspected changes in chromatin architecture. Acetylation of histones at lysine residues effectively neutralizes positive charge and leads to chromatin de-condensation [44]. We examined the magnitude of lysine acetylation in patterned and non-patterned cells and see a significant decrease in global lysine acetylation in both star-patterned and pentagon-patterned MSCs when compared to non-patterned MSCs. We also examined several specific marks including H3K9me3, a hallmark of heterochromatin [45], H3K9ac, an indicator of active promoters [46], and H3K36me2, an indicator of gene transcription [47]. Immunofluorescence staining of patterned versus non-patterned MSCs demonstrates decreased acetylation and methylation marks in micropatterned cells indicating a chromatin state which is less actively transcribed than non-patterned cells.

To further investigate the regulation of chromatin state, we examined the expression level of class 1 histone deacetylases (Fig. 4b). There is no change in HDAC1 expression across conditions, while HDAC2 shows significantly higher expression in non-patterned MSCs. HDAC3 shows slightly higher expression for cells cultured in the star geometry. Taken together, these results suggest that single cell confinement regulates chromatin structure and transcription sites, with evidence for HDAC3-mediated deacetylation at H3K9. This results in a less “active”

chromatin as MSCs are primed for a specific role, consistent with previous work demonstrating decreased H3K9 acetylation during differentiation [48].

Discussion

Autologous MSC therapy is considered one of the most promising treatments for cardiovascular disease; however, the majority of cells die during implantation and clinical efficacy has proved variable. Preconditioning MSCs to augment pro-angiogenic potential has been demonstrated through engineering hypoxia or cytokine signaling [7] to program MSCs into an angiogenic mode. In this work, we have demonstrated a biophysical approach to activate MSCs through single-cell cytoskeleton engineering, to reveal a medicinal state which exhibits broad pro-angiogenic potential, enhanced association with model vasculature in vitro, and the formation of new vasculature in ovo.

The observed overall increase in cytokine secretion is consistent with previous reports of enhanced angiogenic secretory profiles of MSCs on stiffer substrates and our previous observation of the abrogation of these effects by restricting MSC spreading on stiff substrates [24, 49]. This overall increase, however, stands in contrast to previous observations of differential modulation of cytokines in responses to changes in substrate mechanics and is more in line with large-scale changes in MSC secretory profile seen through more potent chemical preconditioning or hypoxia treatments [7]. This suggests a “switch” in

phenotype which activates a pro-angiogenic secretory profile. During wound repair, MSCs home toward sites of injury and take on a more active migratory state. This is in contrast to the more quiescent state observed during homeostasis [50, 51].

A proposed trophic response to injury is the “activation” of MSCs into a medicinal state which organizes a regenerative microenvironment, with subsequent stabilization spurred by MSCs reacquiring a more quiescent pericytic phenotype [52, 53]. Activated pro-angiogenic pericytes acquire a more amoeboid morphology, are more migratory, and support endothelial cell proliferation and migration [54]. In all cases, MSCs exhibit remarkably robust and versatile plasticity between different phenotypes to regulate angiogenesis both in vitro and in vivo [34].

Furthermore, perturbation of pericytes’ contractility through Rho-GTPase has been shown to affect regulation of endothelial cell proliferation, with Rho-GTPase-activated cells losing the capability of growth-arresting endothelial cells [30]. In support of a contractility mechanism guiding pericyte activity, Herman and colleagues showed how increasing spreading and actin cytoskeletal organization through MRIP silencing in pericytes promote endothelial cell tubulogenesis in vitro [31]. Interestingly, MSC-derived extracellular vesicles [55] and secretory vesicle transport may be enhanced by coordination of the actin cytoskeleton and polarity of MSCs on patterned substrates [56]. Our observation of higher association of MSCs from star patterns with hMVECs, and higher tube formation in vitro and in ovo coupled with increased CD146 expression, is consistent with the pro-angiogenic behavior observed for CD146-positive MSCs [37]. This evidence, combined with the proposed perivascular source of MSCs [15] and MSC-pericyte plasticity [34], has led us to hypothesize that a cytoskeletal switch induced by microengineering cytoskeletal tension will activate MSCs into a pericytic, pro-angiogenic phenotype.

A pro-angiogenic switch for MSCs promoting paracrine signaling may find clinical application by increasing angiogenesis outcomes regardless of long-term engraftment. Modifying biomaterials to promote a pericytic state may also improve the efficiency of implanted therapies. Further work is, however, required to fully characterize this state, whether it is activated through other pathways, and how it may synergize with other preconditioning strategies for optimal treatment.

Conclusion

We show evidence that engineering the adhesion and cytoskeletal machinery modulates MSC pro-angiogenic activity through actomyosin-based cytoskeletal tension, lysine acetylation, and chromatin remodeling, with subsequent specification of a medicinal, pericytic phenotype. Microengineered

substrates are a useful platform to normalize cell state across a heterogeneous population and may prove a versatile route to “priming” a patient’s cells for medicinal activity prior to therapy.

Acknowledgements This work was supported by the National Heart Lung and Blood Institute of the National Institutes of Health, grant number HL121757. The authors declare no competing financial interests. We would like to thank the Beckman Institute and Institute of Genomic Biology Imaging facilities.

References

1. Mozaffarian D, Benjamin EJ, Go AS, Arnett DK, Blaha MJ, Cushman M, et al. Heart disease and stroke statistics—2015 update: a report from the American Heart Association. *Circulation*. 2015;131:e29–322.
2. Deveza L, Choi J, Yang F. Therapeutic angiogenesis for treating cardiovascular diseases. *Theranostics*. 2012;2:801–14.
3. Zachary I, Morgan RD. Therapeutic angiogenesis for cardiovascular disease: biological context, challenges, prospects. *Heart*. 2011;97:181–9.
4. Carmeliet P, Jain RK. Molecular mechanisms and clinical applications of angiogenesis. *Nature*. 2011;473:298–307.
5. Epstein SE, Kornowski R, Fuchs S, Dvorak HF. Angiogenesis therapy: amidst the hype, the neglected potential for serious side effects. *Circulation*. 2001;104:115–9.
6. Beohar N, Rapp J, Pandya S, Losordo DW. Rebuilding the damaged heart: the potential of cytokines and growth factors in the treatment of ischemic heart disease. *J Am Coll Cardiol*. 2010;56:1287–97.
7. Ranganath SH, Levy O, Inamdar MS, Karp JM. Harnessing the mesenchymal stem cell secretome for the treatment of cardiovascular disease. *Cell Stem Cell*. 2012;10:244–58.
8. Pittenger MF, Mackay AM, Beck SC, Jaiswal RK, Douglas R, Mosca JD, et al. Multilineage potential of adult human mesenchymal stem cells. *Science*. 1999;284:143–7.
9. Wingate K, Bonani W, Tan Y, Bryant SJ, Tan W. Compressive elasticity of three-dimensional nanofiber matrix directs mesenchymal stem cell differentiation to vascular cells with endothelial or smooth muscle cell markers. *Acta Biomater*. 2012;8:1440–9.
10. Pijnappels DA, Schaliij MJ, Ramkisoensing AA, Van Tuyn J, De Vries AA, Van Der Laarse A, et al. Forced alignment of mesenchymal stem cells undergoing cardiomyogenic differentiation affects functional integration with cardiomyocyte cultures. *Circ Res*. 2008;103:167–76.
11. Leiker M. Assessment of a nuclear affinity labeling method for tracking implanted mesenchymal stem cells. *Cell Transplant*. 2008;17:911–22.
12. Ankrum J, Karp JM. Mesenchymal stem cell therapy: two steps forward, one step back. *Trends Mol Med*. 2010;16:203–9.
13. Crisan M, Yap S, Casteilla L, Chen C-W, Corselli M, Park TS, et al. A perivascular origin for mesenchymal stem cells in multiple human organs. *Cell Stem Cell*. 2008;3:301–13.
14. Traktuev DO, Merfeld-Clauss S, Li J, Kolonin M, Arap W, Pasqualini R, et al. A population of multipotent CD34-positive adipose stromal cells share pericyte and mesenchymal surface markers, reside in a periendothelial location, and stabilize endothelial networks. *Circ Res*. 2008;102:77–85.
15. Caplan AI. All MSCs are pericytes? *Cell Stem Cell*. 2008;3:229–30.

16. Mills SJ, Cowin AJ, Kaur P. Pericytes, mesenchymal stem cells and the wound healing process. *Cells*. 2013;2:621–34.
17. da Silva ML, Caplan AI, Nardi NB. In search of the in vivo identity of mesenchymal stem cells. *Stem Cells*. 2008;26:2287–99.
18. Koike N, Fukumura D, Gralla O, Au P, Schechner JS, Jain RK. Tissue engineering: creation of long-lasting blood vessels. *Nature*. 2004;428:138–9.
19. Engler AJ, Sen S, Sweeney HL, Discher DE. Matrix elasticity directs stem cell lineage specification. *Cell*. 2006;126:677–89.
20. Lee J, Abdeen AA, Zhang D, Kilian KA. Directing stem cell fate on hydrogel substrates by controlling cell geometry, matrix mechanics and adhesion ligand composition. *Biomaterials*. 2013;34:8140–8.
21. Li Y, Kilian KA. Bridging the gap: from 2D cell culture to 3D microengineered extracellular matrices. *Adv Healthc Mater*. 2015;4:2780–96.
22. Kilian KA, Bugarija B, Lahn BT, Mrksich M. Geometric cues for directing the differentiation of mesenchymal stem cells. *Proc Natl Acad Sci*. 2010;107:4872–7.
23. Zhang D, Kilian KA. The effect of mesenchymal stem cell shape on the maintenance of multipotency. *Biomaterials*. 2013;34:3962–9.
24. Abdeen AA, Weiss JB, Lee J, Kilian KA. Matrix composition and mechanics direct proangiogenic signaling from mesenchymal stem cells. *Tissue Eng Part A*. 2014;20:2737–45.
25. Krock BL, Skuli N, Simon MC. Hypoxia-induced angiogenesis: good and evil. *Genes Cancer*. 2011;2:117–33.
26. Johnson KE, Wilgus TA. Vascular endothelial growth factor and angiogenesis in the regulation of cutaneous wound repair. *Adv wound care*. 2014;3:647–61.
27. Mammoto A, Connor KM, Mammoto T, Yung CW, Huh D, Aderman CM, et al. A mechanosensitive transcriptional mechanism that controls angiogenesis. *Nature*. 2009;457:1103–8.
28. Chen W, Frangogiannis NG. Fibroblasts in post-infarction inflammation and cardiac repair. *Biochim Biophys Acta - Mol Cell Res*. 1833;2013:945–53.
29. Darby I, Skalli O, Gabbiani G. α -smooth muscle actin is transiently expressed by myofibroblasts during experimental wound healing. *Lab Invest*. 63:21–9.
30. Kutcher ME, Kolyada AY, Surks HK, Herman IM. Pericyte Rho GTPase mediates both pericyte contractile phenotype and capillary endothelial growth state. *Am J Pathol American Society for Investigative Pathology*. 2007;171:693–701.
31. Durham JT, Surks HK, Dulmovits BM, Herman IM. Pericyte contractility controls endothelial cell cycle progression and sprouting: insights into angiogenic switch mechanics. *AJP Cell Physiol*. 2014;307:C878–92.
32. Théry M. Micropatterning as a tool to decipher cell morphogenesis and functions. *J Cell Sci*. 2010;123:4201–13.
33. Lee J, Abdeen AA, Tang X, Saif TA, Kilian KA. Geometric guidance of integrin mediated traction stress during stem cell differentiation. *Biomaterials*. 2015;69:174–83.
34. Kelly-goss MR, Sweat RS, Stapor PC, Peirce SM, Murfee WL. Targeting pericytes for angiogenic therapies. *Microcirculation*. 2014;21:345–57.
35. Mitchell TS, Bradley J, Robinson GS, Shima DT, Ng YS. RGS5 expression is a quantitative measure of pericyte coverage of blood vessels. *Angiogenesis*. 2008;11:141–51.
36. Berger M, Bergers G, Arnold B, Hammerling GJ, Ganss R. Regulator of G-protein signaling-5 induction in pericytes coincides with active vessel remodeling during neovascularization. *Blood*. 2005;105:1094–101.
37. Blocki A, Wang Y, Koch M, Peh P, Beyer S, Law P, et al. Not all MSCs can act as pericytes: functional in vitro assays to distinguish pericytes from other mesenchymal stem cells in angiogenesis. *Stem Cells Dev*. 2013;22:2347–55.
38. Shi YU, Li H, Zhang X, Fu Y, Huang YAN, Po P, et al. Continuous cyclic mechanical tension inhibited Runx2 expression in mesenchymal stem cells through RhoA-ERK1/2 pathway. *J Cell Physiol*. 2011;226:2159–69.
39. Ponce ML, Kleinmann HK. The chick chorioallantoic membrane as an in vivo angiogenesis model. *Curr. Protoc. Cell Biol*. 2003;Chapter 19:Unit 19.5.
40. Wang N, Tytell JD, Ingber DE. Mechanotransduction at a distance: mechanically coupling the extracellular matrix with the nucleus. *Nat Rev Mol Cell Biol*. 2009;10:75–82.
41. Versaevol M, Grevesse T, Gabriele S. Spatial coordination between cell and nuclear shape within micropatterned endothelial cells. *Nat Commun*. 2012;3:671.
42. Jain N, Iyer KV, Kumar A, Shivashankar GV. Cell geometric constraints induce modular gene-expression patterns via redistribution of HDAC3 regulated by actomyosin contractility. *Proc Natl Acad Sci*. 2013;110:3–8.
43. Le Beyec J, Xu R, Lee S-Y, Nelson CM, Rizki A, Alcaraz J, et al. Cell shape regulates global histone acetylation in human mammary epithelial cells. *Exp Cell Res*. 2007;313:3066–75.
44. Struhl K. Histone acetylation and transcriptional regulatory mechanisms. *Genes Dev*. 1998;12:599–606.
45. Peters AHFM, O'Carroll D, Scherthan H, Mechtler K, Sauer S, Schöfer C, et al. Loss of the Suv39h histone methyltransferases impairs mammalian heterochromatin and genome stability. *Cell*. 2001;107:323–37.
46. Karmodiya K, Krebs AR, Oulad-Abdelghani M, Kimura H, Tora L. H3K9 and H3K14 acetylation co-occur at many gene regulatory elements, while H3K14ac marks a subset of inactive inducible promoters in mouse embryonic stem cells. *BMC Genomics*. 2012;13:424.
47. Rao B, Shibata Y, Strahl BD, Lieb JD. Dimethylation of histone H3 at lysine 36 demarcates regulatory and nonregulatory chromatin genome-wide. *Mol Cell Biol*. 2005;25:9447–59.
48. Krejci J, Uhlířová R, Galiová G, Kozubek S, Smigová J, Bártová E. Genome-wide reduction in H3K9 acetylation during human embryonic stem cell differentiation. *J Cell Physiol*. 2009;219:677–87.
49. Seib FP, Prewitz M, Werner C, Bornhäuser M. Matrix elasticity regulates the secretory profile of human bone marrow-derived multipotent mesenchymal stromal cells (MSCs). *Biochem Biophys Res Commun*. 2009;389:663–7.
50. Rustad KC, Gurtner GC. Mesenchymal stem cells home to sites of injury and inflammation. *Adv Wound Care*. 2012;1:147–52.
51. Murphy MB, Moncivais K, Caplan AI. Mesenchymal stem cells: environmentally responsive therapeutics for regenerative medicine. *Exp Mol Med*. 2013;45:e54.
52. Caplan AI, Correa D. The MSC: an injury drugstore. *Cell Stem Cell*. 2011;9:11–5.
53. Stratman AN, Malotte KM, Mahan RD, Davis MJ, Davis GE. Pericyte recruitment during vasculogenic tube assembly stimulates endothelial basement membrane matrix formation. *Blood*. 2009;114:5091–101.
54. Díaz-Flores L, Gutiérrez R, Madrid JF, Varela H, Valladares F, Acosta E, et al. Pericytes. Morphofunction, interactions and pathology in a quiescent and activated mesenchymal cell niche. *Histol Histopathol*. 2009;24:909–69.
55. Merino-gonzález C, Zuñiga FA, Escudero C, Ormazabal V, Reyes C, Nova-lamperti E, et al. Mesenchymal stem cell-derived extracellular vesicles promote angiogenesis: potential clinical application. *Front Physiol*. 2016;7:1–9.
56. DePina AS, Langford GM. Vesicle transport: the role of actin filaments and myosin. *Microsc Res Tech*. 1999;47(2):93–106.